Impact of longitudinal power budget in coherent transmission systems employing digital back-propagation

Danish Rafique* and Andrew D. Ellis

Photonics Systems Group, Tyndall National Institute and Department of Electrical Engineering/Physics, University College Cork, Dyke Parade, Prospect Row, Cork, Ireland
*danish.rafique@tyndall.ie

Abstract: We report the impact of longitudinal signal power profile on the transmission performance of coherently-detected 112 Gb/s m-ary polarization multiplexed quadrature amplitude modulation system after compensation of deterministic nonlinear fibre impairments. Performance improvements up to 0.6 dB (Q_{eff}) are reported for a non-uniform transmission link power profile. Further investigation reveals that the evolution of the transmission performance with power profile management is fully consistent with the parametric amplification of the amplified spontaneous emission by the signal through four-wave mixing. In particular, for a non-dispersion managed system, a single-step increment of 4 dB in the amplifier gain, with respect to a uniform gain profile, at ~2/3rd of the total reach considerably improves the transmission performance for all the formats studied. In contrary a negative-step profile, emulating a failure (gain decrease or loss increase), significantly degrades the bit-error rate.

OCIS codes: (060.1660) Coherent communications; (060.4370) Nonlinear optics, fibers.

References and links

1. A. D. Ellis, J. Zhao, and D. Cotter, "Approaching the non-linear Shannon limit," J. Lightwave Technol. **28**(4), 423–433 (2010).
2. A. R. Chraplyvy, "Limitations on lightwave communications imposed by optical-fiber nonlinearity," J. Lightwave Technol. **8**(10), 1548–1557 (1990).
3. D. Marcuse, A. R. Chraplyvy, and R. W. Tkach, "Effect of fiber nonlinearity on long-distance transmission," J. Lightwave Technol. **9**(1), 121–128 (1991).
4. X. Zhou, E. F. Mateo, and G. Li, "Fiber nonlinearity management – from carrier perspective," Optical Fiber Communication Conference, OFC '11, NThB4, (2011).
5. C. Weber, C.-A. Bunge, and K. Petermann, "Fiber nonlinearities in systems using electronic predistortion of dispersion at 10 and 40 Gbit/s," J. Lightwave Technol. **27**(16), 3654–3661 (2009).
6. D. Rafique, J. Zhao, and A. D. Ellis, "Digital back-propagation for spectrally efficient WDM 112 Gbit/s PM m-ary QAM transmission," Opt. Express **19**(6), 5219–5224 (2011).
7. E. Ip, "Nonlinear compensation using backpropagation for polarization-multiplexed transmission," J. Lightwave Technol. **28**(6), 939–951 (2010).
8. D. Rafique and A. D. Ellis, "Impact of signal-ASE four-wave mixing on the effectiveness of digital back-propagation in 112 Gb/s PM-QPSK systems," Opt. Express **19**(4), 3449–3454 (2011).
9. A. Mecozzi, "On the optimization of the gain distribution of transmission lines with unequal amplifier spacing," IEEE Photon. Technol. Lett. **10**(7), 1033–1035 (1998).
10. I. Nasieva, J. D. Ania-Castanon, and S. K. Turitsyn, "Nonlinearity management in fibre links with distributed amplification," Electron. Lett. **39**(11), 856–857 (2003).
11. A. P. T. Lau and J. M. Kahn, "Power profile optimization in phase-modulated systems in presence of nonlinear phase noise," IEEE Photon. Technol. Lett. **18**(23), 2514–2516 (2006).
12. P. J. Winzer, A. H. Gnauck, C. R. Doerr, M. Magarini, and L. L. Buhl, "Spectrally efficient long-haul optical networking using 112-Gb/s polarization-multiplexed 16-QAM," J. Lightwave Technol. **28**(4), 547–556 (2010).
13. S. Makovejs, D. S. Millar, V. Mikhailov, G. Gavioli, R. I. Killey, S. J. Savory, and P. Bayvel, "Experimental investigation of PDM-QAM16 transmission at 112 Gbit/s over 2400 km," Optical Fiber Communication Conference, OFC '10, OMJ6, (2010).
14. T. Pfau, S. Hoffmann, and R. Noé, "Hardware-efficient coherent digital receiver concept with feedforward carrier recovery for *M*-QAM constellations," J. Lightwave Technol. **27**(8), 989–999 (2009).

15. L. B. Du and A. J. Lowery, "Experimental demonstration of XPM compensation for CO-OFDM systems with periodic dispersion maps," Optical Fiber Communication Conference, OFC'11, OWW2, (2011).
16. D. Rafique, M. Mussolin, M. Forzati, J. Mårtensson, M. N. Chugtai, and A. D. Ellis, "Compensation of intra-channel nonlinear fibre impairments using simplified digital back-propagation algorithm," Opt. Express **19**(10), 9453–9460 (2011).
17. L. Li, Z. Tao, L. Dou, W. Yan, S. Oda, T. Tanimura, T. Hoshida, and J. C. Rasmussen, "Implementation efficient nonlinear equalizer based on correlated digital backpropagation," Optical Fiber Communication Conference, OFC '11, 2011, OWW3.
18. F. Yaman and G. Li, "Nonlinear impairment compensation for polarization-division multiplexed WDM transmission using digital backward propagation," IEEE Photon. J. **2**(5), 816–832 (2010).

1. Introduction

With the ever increasing demand for high information rates and advances in bandwidth intense applications, the available transmission capacity for single mode optical fibre is rapidly approaching its limit [1]. One of the main limitations is the nonlinear behavior of the optical fiber. It may be shown [2, 3] that the effects of four-wave mixing (FWM), self- and cross-phase modulation and other nonlinear effects approximately depend on the path averaged power, and become increasingly pronounced as power levels are increased.

The recent revival of coherent detection with the availability of high speed digital signal processing technologies has enabled electronic mitigation of these effects [4, 5]. In particular, electronic signal processing using digital back-propagation (DBP) has been applied to the compensation of channel nonlinearities [6, 7]. However the performance improvements by single-channel nonlinearity compensation are curtailed by inter-channel nonlinearities [7] and multi-channel compensation is limited by signal-amplified spontaneous emission (ASE) four-wave mixing (SN-FWM) [8]. A rather obvious way to minimize nonlinear impairments is by lowering the signal power, leading to a trade off with the optical signal-to-noise ratio (OSNR) at the receiver. This trade off has previously been studied for unequal amplifier spacing [9], distributed amplification [10], and phase modulated systems [11] where a longitudinal variation in launch power was found to be advantageous. However, to our knowledge there have been no reports on the impact of power profile optimization on the transmission performance of coherent systems, limited by SN-FWM, employing advanced multi-level modulation formats [12, 13] and mitigation of nonlinear fibre impairments via DBP. In context of increasing growth in capacity demands [1], near-future transmission systems employing wide-band DBP would eventually be limited by SN-FWM effects [6, 8].

In this paper, we demonstrate that modifying the longitudinal power distribution by optimizing the gain of just one of the in-line amplifiers may improve the transmission performance for coherently-detected 112 Gb/s m-ary polarization multiplexed quadrature amplitude modulation (PM-mQAM, m=4, 16, 64, 256) transmission employing digital back-propagation. Our results suggest that if the gain of the in-line optical amplifiers is set to exactly compensate for uniform fibre loss, an increase (~4 dB) in the amplifier gain at ~2/3rd of the total reach improves the performance of the overall system, consistent with the theoretical predictions based on SN-FWM. In particular, for systems whose length is such that the bit error rate (BER) at the optimum uniform launch power would be ~1.5×10^{-3} (Q_{eff} of ~9.5 dB), Q_{eff} increases by 0.6 dB and enables over 1 dB reduction in transmitted power (power launched into the first fibre segment) for all formats studied. Furthermore, we report that with a fixed received OSNR, if a fault is encountered anywhere along the link, the transmission performance is always degraded.

3. Transmission model

Figure 1 shows the simulation setup employed using VPItransmissionMaker®v8.5 for transmission and MATLAB®v7.10 for signal processing. The 112 Gb/s PM-mQAM transmitter consisted of a continuous-wave laser operating at 1550 nm, followed by two Mach-Zehnder structure based I-Q modulators for x- and y-polarizations. 4, 16, 64 and 256 order PM-mQAM modulation formats were employed at a constant bit-rate of 112 Gb/s, i.e. with baud-rates of 28 Gbaud, 14 Gbaud, 9.33 Gbaud and 7 Gbaud, respectively. Each transmitter encoded two independent pseudo-random bit sequences (PRBS), one for each

polarization, each de-multiplexed separately into two sampled multi-level output symbol streams which were used to modulate an in-phase and a quadrature phase carrier, respectively. The simulation conditions ensured 16 samples/symbol, with 2^{13} total transmitted symbols per polarization per channel. The 112 Gb/s PM-mQAM signal was propagated over a non-dispersion managed link using single-stage optical amplifiers. The link comprised $M \times 80$km spans of standard single mode fibre (SSMF) for transmission. The amplifiers were modelled with a 4.5 dB noise figure and 16 dB gain. For simplicity, we neglected the effects of polarization mode dispersion and laser line-width in this paper (for the worst-case scenario employing 256QAM, 80 kHz line-width can be tolerated [14]). The fibre had attenuation (α) of 0.2 dB/km, dispersion (D) of 20 ps/nm.km, and a nonlinearity coefficient (γ) of 1.4/W.km.

In order to emulate a single-step increment/decrement in transmission link power profile, an additional amplification/attenuation stage was employed after N spans, as shown in Fig. 2. To focus on the nonlinear effects, we initially maintained a constant received OSNR for all configurations, so a step increase in launch power at $(N+1)^{th}$ span, i.e. positive-step, resulted in a decrease in launch power (red triangle, ΔP_1^-) for the first N spans, and an increase (red triangle, ΔP_2^+) for the remaining M-N spans and vice versa. It is worth noticing that this approach is suitable for the upgrade of existing systems, since in real transmission links, the amplifiers would be command-controlled, allowing for power-profile adjustment.
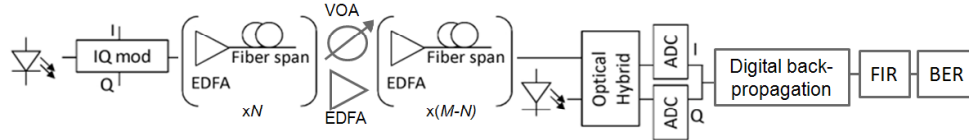

Fig. 1. Simulation setup for 112 Gb/s PM-mQAM (m=4, 16, 64, 256) transmission system with M total spans (step after N^{th} span).

After fiber transmission, the received signal was demultiplexed, pre-amplified and coherently-detected using a local oscillator to give baseband electrical signal, and down sampled to 2 samples per symbol. Transmission impairments were compensated via digital back-propagation (DBP), which was numerically implemented by up-sampling the received signal to 16 samples per symbol and reconstructing the optical field from the inphase and quadrature components, followed by a split-step Fourier method based solution of nonlinear Schrödinger equation. Although various simplifications of DBP algorithm have been proposed lately [15–17], in order to determine the maximum potential performance of the power-profile management, the step-size was chosen adaptively such that in each step the change in phase of the optical field was no more than 0.05 degrees. Note that transmission performance reported here may reduce given a coarse-step DBP is employed [13, 18].
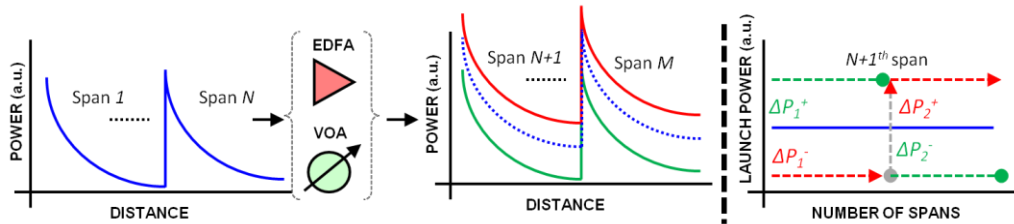

Fig. 2. Left: Transmission link power profile as a function of transmission distance. A positive or negative step in the power profile is ensured with an EDFA or a passive attenuator element, respectively. Right: Negative (circle) or Positive (triangle) step at $N+1^{th}$ span, ensuring a fixed received OSNR by launching high or low power, respectively.

Residual distortion and any bandwidth limitations were compensated with a receiver amplitude response implemented using FIR filters (fractionally-spaced taps), and polarization de-multiplexing was then performed using a butterfly structure, where filters were adapted using a least mean square algorithm. Note that no carrier phase recovery was required since

laser linewidth was neglected in this study. Finally, the symbol decisions were made, and the performance assessed by direct error counting (converted into an effective Q-factor (Q_{eff})).
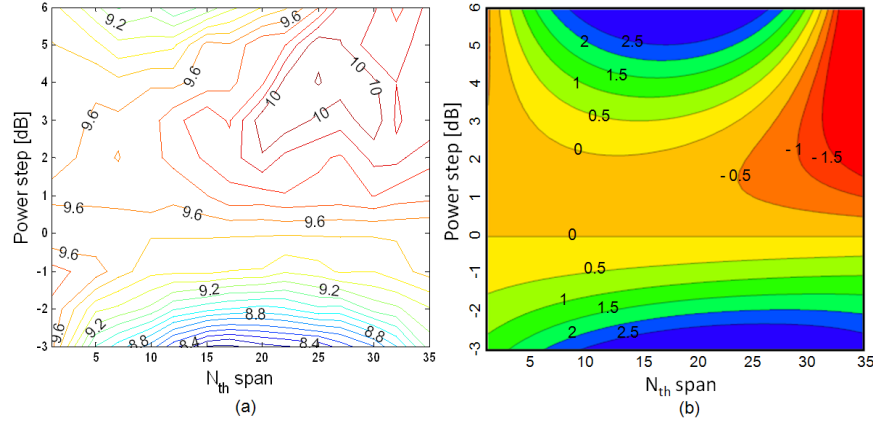

Fig. 3. Performance of PM-64QAM at a transmission distance of 3,200 km (40 spans) after DBP. Contour curves represent a) Q_{eff} and, b) FWM power, as a function of position and gain/loss of power profile shaping element. Received OSNR is fixed to 24.4 dB for all the configurations.

3. Results and discussions

We first consider the performance of PM-64QAM after transmission over 3,200 km (40 spans) with DBP. We fix the reference launch power at the optimum launch power for a uniform power profile, where we observe a Q_{eff} of 9.5 dB (BER of 1.4×10^{-3}) and a received OSNR of 24.4 dB. This configuration is referred to as conventional power profile. Figure 3(a) plots the calculated Q_{eff} (contour curves) as a function of the position and gain/loss of the node containing the power step, for a fixed received OSNR. It can be seen that when positive-step is employed, the transmission performance may improve for any given position of the additional gain element. From the plot, one can clearly locate an optimum region from 20th span to 30th span with a positive step size of ~3-4 dB. In particular, the best map can be identified when the amplifier is placed after the 25th span and a gain of 4 dB is employed, enabling a 0.6 dB Q_{eff} improvement. In general performance improvement is obtained for a wide range of power steps provided the step is located after the midpoint of the system. On the other hand, the figure also shows that given a negative-step profile is employed, emulating an amplification stage failure or an increase in fibre loss, the transmission performance is always degraded, even if the OSNR is restored by adjusting the transmitter launch power.

In order to gain insight into the physical phenomenon behind the optimum power profile we considered the parametric amplification of noise by the signal, treating the contribution from each amplifier as an independent random variable, with Gaussian statistics, such that the additional noise power spectral density is given by [8],

$$I_{Total}{}^2 = \sum_{m=1}^{N} \left(I_{FWM(1)}\right)^2 + s \sum_{m=N+1}^{M} \left(I_{FWM(2)}\right)^2 \qquad (1a)$$

$$I_{FWM(x)} = m I_{noise} . I_{signal(x)}{}^2 \left(K_1 + K_2 + \left\{Log\left(m\right) - 1 + 1/m\right\} K_3\right) \qquad (1b)$$

$$K_1 = \gamma^2 / (\pi^2 |\beta_2| \alpha), K_2 = K_1 \ln\left(2\pi^2 B^2 |\beta_2| / \alpha\right) \pi, K_3 = 2\pi K_1 / (\alpha L) \qquad (1c)$$

where $I_{signal(x\,=\,1,2)}$ is the signal power spectral density for the first half and second half of the link, respectively, s represents the step employed, I_{noise} is the noise power spectral density from a single amplifier. K_1 term and K_2 plus K_3 terms represent weakly and strongly phase matched regimes respectively. N is the number of spans in first half of the link, M is the total

number of spans, B is signal bandwidth, γ the nonlinearity coefficient, α is the fibre loss and β_2 the group velocity dispersion (terms proportional *to K_3* were neglected since $K_3 \ll K_2$). We plot the change in SN-FWM power after DBP (contour lines) in Fig. 3(b) (similar conditions as to Fig. 3(a)), and one can clearly observe an excellent agreement between the numerical data (Fig. 3(a)) and theoretical predictions (Fig. 3(b)), where the overall trends are accurately predicted by a signal-ASE FWM process (where SN-FWM may limit both single- and multi-channel transmission systems, employing wide-band DBP [6]). Note that these trends are apparent due to the super-linear length dependence of SN-FWM (see Eq. (1a), Eq. (1b) and Eq. (1c)), and for other nonlinear regimes, such as cross-phase modulation and four-wave mixing which have linear or sub-linear length scaling, we would anticipate reductions in the impact of longitudinal power profiling. One key point to note here is that whilst DBP reverses the effect of deterministic nonlinear fibre impairments, the effect on nonlinear effects incorporating noise are somewhat different. This phenomenon is intuitively shown in Fig. 4 which plots the signal and noise power profiles as a function of distance. It can be seen that the signal power profile is reversed as expected. With regard to the noise effects, note that due to the ASE build-up in forward propagation, the back-propagating signal essentially sees noise from all the amplifiers. Now, the nonlinear noise (SN-FWM) only builds up for few spans in the forward transmission link, therefore in DBP, the nonlinear noise terms are first compensated (negative γ) up to the accumulated amplifier noise, and then new nonlinear noise terms are added since digital parametric amplification of noise is unavoidable due to excess amplifier noise seen by the signal which is back-propagated.
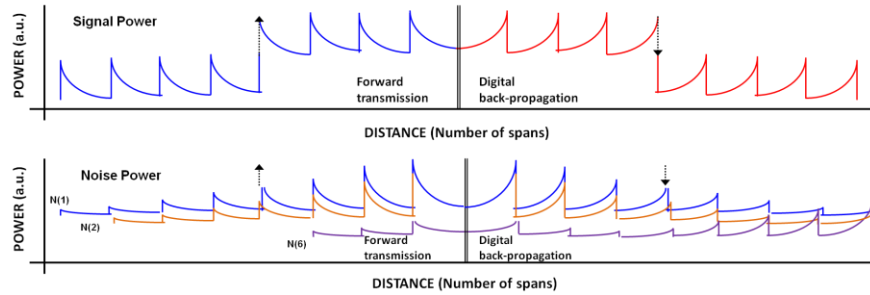

Fig. 4. Link power profile as a function of transmission distance for an 8 span system. Signal power profile (top), noise power profile (bottom, zero offset for each curve), where N(1,2,6) represent various noise terms. The arrow represents gain element (up) for forward transmission, and loss element (down) for digital back-propagation.
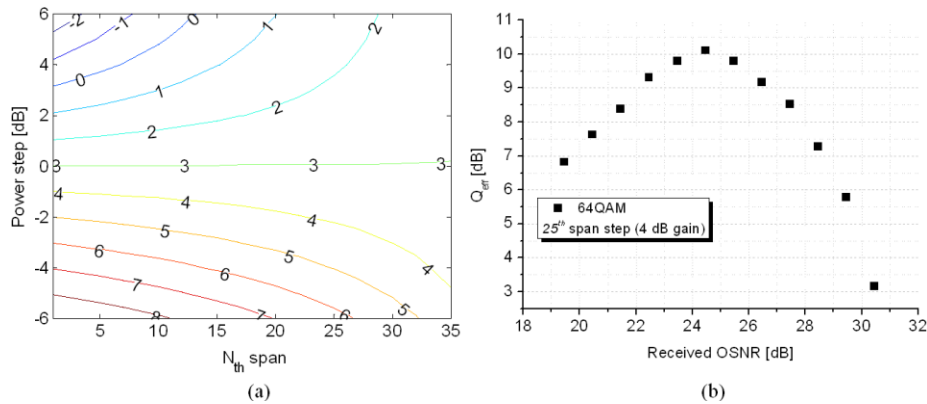

Fig. 5. Performance of PM-64QAM at a transmission distance of 3,200 km (40 spans) after DBP. a) Contour curves represent launch power as a function of position and gain/loss of power profile shaping element; b) Q_{eff} as a function of OSNR for the optimum profile with a gain of 4 dB after the 25th span.

Figure 5(a) plots the required transmitter launch power for various configurations in Fig. 3. It can be seen that for positive-step profile, the launch power is always lower than conventional power profile, and a 1.1 dB reduction in launch power can be seen for the optimum power profile. This system is limited by the overall signal to noise ratio, including the parametrically amplified noise (Eq. (1)). Consequently the optimum configuration may be understood from the relative impacts of the signal power and transmission length in Eq. (1). In the optimum configuration, the signal power is reduced for part of the transmission length, and is increased for the remainder. Where the signal power is reduced, the quadratic dependence of the parametric gain on signal power ensures that the contribution from this section is reduced. On the other hand, where the signal power is increased, fewer spans are included, thereby strongly mitigating the impact of the increased signal power, and resulting in an optimum step size for a given step location.

Figure 5(b) plots the Q_{eff} as a function of received OSNR for the optimum profile with a gain of 4 dB and a fixed step after the 25th span for PM-64QAM. It can be seen that the Q_{eff} curve follows the well-known optimum launch power phenomenon, where at lower launch powers, the system performance is limited by noise and the performance peaks at an optimum OSNR. The figure depicts an important design criterion and shows that even with the new optimum power profile, the optimum OSNR is consistent with that of conventional power profile.

In order to verify the validity of our results for a range of modulation formats, we optimized the power profiles for PM-mQAM formats via full numerical contour search similar to Fig. 3. In order to enable a fair comparison across the formats, reaches were adjusted to give Q_{eff} of ~9.5 at the optimum launch power for a uniform power profile resulting in transmission distances of 1,280 km (256QAM), 3,200 km (64QAM), 8,400 km (16QAM), and 21,840 km (4QAM). It is found that the optimum power profile is similar to that of Fig. 3, across the family of QAM transmission schemes. Figure 6 shows the performance of PM-mQAM both for the optimum power profile and a negative-step profile, at 2/3rd of the total reach for each modulation format. It can be seen that when negative-step is employed the performance degrades severely compared to the conventional power profile, regardless of the modulation format, where slightly greater penalties are observed for lower-order formats. In contrary, with positive-step profile, Q_{eff} improvements are observed across all the formats, however with reduced improvement for PM-256QAM due to the significantly reduced system length, which reduces the impact of the nonlinear length dependence of the noise amplification.
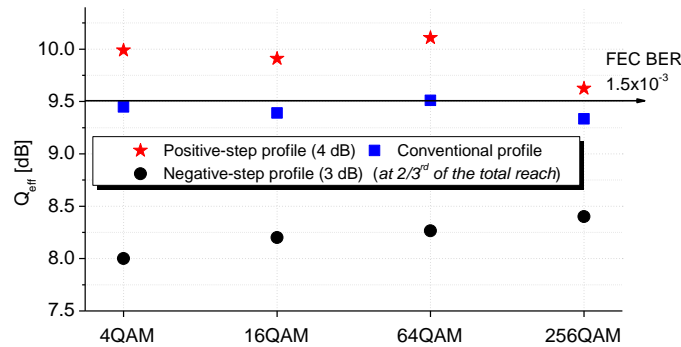

Fig. 6. Q_{eff} for PM-mQAM at transmission distances of 1,280 km (256QAM), 3,200 km (64QAM), 8,400 km (16QAM), and 21,840 km (4QAM), a) Positive-step profile (4 dB, at 2/3rd of the total reach), b) Negative-step profile (3 dB, at 2/3rd of the total reach), a) Conventional power profile (launched power = received power).

4. Conclusion

We have demonstrated that the longitudinal signal power profile along a transmission link can be effectively designed to reduce the nonlinear penalties in a coherently-detected 112 Gb/s PM-mQAM system employing digital back-propagation. We have qualitatively confirmed that our simulation results are consistent with analytical predictions of the dominant nonlinear effect (signal-noise four-wave mixing in this case). In particular, performance improvements up to 0.6 dB have been reported for an optimized power profile with a single-step amplifying stage (4 dB) positioned at $2/3^{rd}$ of the total transmission reach for a variety of modulation formats, enabling BER at FEC threshold of 1.5×10^{-3}. More complex power profile optimization involving greater than one amplifier would be the subject of a subsequent study. In the view of near future optical network deployments, we believe that single/multi-step power profile optimization would significantly improve the transmission performance.